Published in final edited form as:
Plast Reconstr Surg. 2012 April ; 129(4): 825–834. doi:10.1097/PRS.0b013e3182450b2d.

Regulation of Adipogenesis by Lymphatic Fluid Stasis Part I: Adipogenesis, Fibrosis, and Inflammation

Jamie C. Zampell, MD[1], **Seth Aschen**[1], **Evan S. Weitman, MD**[1], **Alan Yan**[1], **Sonia Elhadad, PhD**[1], **Marina De Brot Andrade, MD**[2], and **Babak J. Mehrara, MD, FACS**[1]

[1]The Division of Plastic and Reconstructive Surgery, Memorial Sloan-Kettering Cancer Center, New York, NY 10065

[2]The Division of Breast Surgery, Department of Surgery, Memorial Sloan-Kettering Cancer Center, New York, NY 10065

Abstract

Background—Although fat deposition is a defining clinical characteristic of lymphedema, the cellular mechanisms that regulate this response remain unknown. The goals of this two-part study were to determine the effect of lymphatic fluid stasis on adipogenesis and inflammation (part 1) and how these changes regulate the temporal and spatial expression of fat differentiation genes (part 2).

Methods—Adult female mice underwent tail lymphatic ablation and were sacrificed 6 weeks after surgery (n=20). Fat deposition, fibrosis, and inflammation were then analyzed in the regions of the tail exposed to lymphatic fluid stasis as compared with normal lymphatic flow.

Results—Lymphatic fluid stasis in the tail resulted in significant subcutaneous fat deposition with a 2-fold increase in fat thickness ($p<0.01$). In addition, lymphatic stasis was associated with subcutaneous fat fibrosis and collagen deposition. Adipogenesis in response to lymphatic fluid stasis was associated with a marked mononuclear cell inflammatory response (5-fold increase in CD45+ cells; $p<0.001$). In addition, we noted a significant increase in the number of monocytes/macrophages as identified by F4/80 immunohistochemistry ($p<0.001$).

Conclusions—The mouse-tail model has pathological findings that are similar to clinical lymphedema including fat deposition, fibrosis, and inflammation. Adipogenesis in response to lymphatic fluid stasis closely resembles this process in obesity. This model therefore provides an excellent means to study the molecular mechanisms that regulate the pathophysiology of lymphedema.

Keywords

Lymph Stasis; inflammation; fibrosis; adipogenesis; macrophage

Introduction

Lymphedema is a chronic disorder that, in Western countries, develops most commonly after injury to the lymphatic system during the course of cancer treatment.(1, 2) Remarkably, it is estimated that as many as 50% of patients who undergo lymph node dissection will go on to develop lymphedema.(3) However, despite the fact that

Correspondence: Babak J. Mehrara, MD FACS, 1275 York Avenue, Suite MRI 1005, New York, NY 10021, 212-639-8639, 212-717-3677 (fax), mehrarab@mskcc.org.

Disclosures: None of the authors have any conflicts of interests or relevant disclosures to the findings presented in this study.

lymphedema is common, treatment remains palliative in nature and is designed primarily to prevent disease progression rather than achieve a cure. As a result, lymphedema serves not only as a source of physical deformity and morbidity, but also a persistent reminder of cancer diagnosis with associated psychological morbidity.(4, 5)

Development of targeted treatments that may prevent or treat lymphedema has been hampered by the lack of animal models. This deficiency has served as a significant barrier for elucidation of the molecular mechanisms that regulate the etiology of lymphedema. As a result, it remains unknown how lymphatic injury results in the clinical findings of fat deposition, chronic inflammation, and fibrosis. Similarly, although obesity and post-operative weight gain are known significant risk factors for lymphedema, it remains unknown how adipogenesis plays a role in the development of lymphedema.

Therefore, the goals of this two-part study were to use a mouse tail model of lymphatic fluid stasis to study adipogenesis and inflammation (part 1) and determine how these changes regulate the temporal and spatial expression of fat differentiation genes (part 2). In this study, we show in the mouse tail model that sustained lymphatic fluid stasis markedly increases fat deposition as a result of adipocyte hypertrophy and an increased number of adipocytes, a pathologic finding evident in clinical lymphedema. In addition, similar to clinical lymphedema, we found that lymphatic fluid stasis in the mouse tail model results in fat fibrosis and inflammation consisting of mononuclear cells and macrophages. Taken together, our results suggest that lymphatic fluid stasis in the mouse tail, similar to clinical lymphedema, results in adipogenesis, fibrosis, and inflammation. The use of the tail model therefore enables detailed molecular analysis of the events that regulate the pathology of lymphedema providing insights into potential treatment or preventative options.

Methods

Mouse tail model

We used our previously described mouse-tail model to examine the effects of lymphatic fluid stasis on adipogenesis, fibrosis, and inflammation.(6–9) Briefly, in order to disrupt superficial lymphatic vessels, we excised a 2mm full thickness circumferential segment of skin from the mid-portion (20mm from the base of the tail) of 8–10 week old female C57BL/6 mice (n=20; Jackson Laboratory, Bar Harbor, Me). Using a dissecting microscope (StereoZoom SZ-4; Leica, Wetzlar, Germany), we identified and ligated deep collecting lymphatics adjacent to the lateral tail veins (Figure 1). Wounds were then covered with a Tegaderm dressing (3M, St. Paul, MN) for 5 days after which they were left open. Based on our previous studies demonstrating progressive inflammation and fibrosis 6 weeks post-operatively, animals were sacrificed for analysis at this time point.(6–9)

Histology and morphometric analysis

Histology—To evaluate tissues exposed to normal lymphatic flow or lymphatic fluid stasis, we harvested cross-sectional segments of the tail 20mm proximal to, or 20 and 30 mm distal to the zone of lymphatic obstruction (designated as $P^{-}20$, $D^{+}20$, and $D^{+}30$; Figure 1). We have shown that this procedure results in lymphatic fluid stasis in the distal tail and that harvesting tissues located well away from the wound (20–30mm) minimizes the effects of inflammatory reactions secondary to wound healing.(7–9) This approach enables us to directly analyze the effects of lymphatic fluid stasis since the proximal portion of the tail has uninterrupted interstitial fluid flow, while the distal region is exposed to lymphatic fluid stasis.

Sections were fixed in 4% paraformaldehyde, decalcified in Immunocal (Decal Chemical Corp, Tallman, NY), embedded in paraffin, and sectioned at 5 μm in thickness. Additional tail sections were similarly fixed and decalcified, but were embedded in Optimum Cutting Temperature media (OCT; Tissue-Tek, Hatfield, PA) and sectioned at 8–10 μm for fresh frozen analysis.

Hematoxylin and Eosin as well as trichrome staining were performed using standard techniques. Oil red O staining was performed on frozen sections to visualize lipid droplets. Briefly, frozen sectioned slides were air dried and submerged in a 0.5% solution of oil red o in propylene glycol followed by washes in graded propylene glycol solutions, and counter-stained with Harris hematoxylin (Dako). Analysis was performed using bright field microscopy (Axioskop 40, Carl Zeiss) and images were obtained using AxioVision imaging software (Carl Zeiss).

Fat Thickness Measurements—To quantify fat deposition in various tail regions, the thickness of the subcutaneous adipose layer was measured using ImageJ software (software available at http://rsweb.nih.gov/ij/) in cross-sectional specimens obtained 20mm proximal ($P^{-}20$) and 20 or 30 mm distal ($D^{+}20$ and $D^{+}30$mm) to the zone of lymphatic obstruction in sections harvested 6 weeks after surgery. Measurements were performed in sections obtained from 5 animals by 2 blinded reviewers in a minimum of 3 high powered fields (10x) per animal.

Immunohistochemistry—Immunohistochemical (IHC) staining was performed to localize type I collagen as well as inflammatory cell markers using our previously published methods.(6) Briefly, slides were deparaffinized in Histochoice clearing agent (Sigma Aldrich, Saint Louis, MO), dehydrated in graded alcohol, and incubated in 0.3% Triton X-100 (Sigma). Antigen retrieval was achieved with boiling 10mM citric acid and endogeous peroxidase activity was quenched with 3.0% hydrogen peroxide followed by blocking with 20% normal serum in 0.1M glycine/0.2% BSA/PBS at 37°C. Sections were then incubated with rabbit polyclonal antibodies for collagen type I (Abcam, Cambridge, MA), rat monoclonal antibodies against CD45 (a pan-leukocyte antigen; R&D systems, Minneapolis, MN), or rat monoclonal antibodies against F4/80 (a monocyte/macrophage marker; Abcam). Control sections were incubated without primary antibody. Staining was detected using biotinylated secondary antibodies and avidin-peroxidase complex (Vectastain ABC kit, Vector Laboratories) followed by visualization with 3,3′ diaminobenzidine tetrahydrochloride (Dako, Carpinteria, CA). Slides were counterstained with Harris hematoxylin (Dako), dehydrated, and mounted. Tissue sections were visualized using bright-field microscopy (Axioscope 40, Carl Zeiss, Germany) and images captured using a Mirax slide scanner (Carl Zeiss). We stained both longitudinal and cross-sections to examine effects of wound healing and gradients of lymphatic stasis on expression of fat differentiation genes.

In order to quantify CD45 or F4/80 staining, 2 blinded reviewers counted the number of positively stained cells in 6–7 high-powered fields (hpf, 40X) per tissue section (n=5 animals per group) in cross-sectional specimens obtained from various regions of the wound. In addition, a trained pathologist (MDB) evaluated the slides for identification of cell types that expressed CD45 and F4/80.

Statistical analysis

Statistical analysis of multiple groups was performed using one-way ANOVA with the Tukey-Kramer multiple comparison *post-hoc* test with $p<0.05$ considered significant. Results are reported as mean ± standard deviation unless otherwise noted.

Results

Lymph stasis increases subcutaneous fat deposition

Similar to our previous observations and consistent with histological findings of clinical lymphedema, we found that distal regions of the mouse tail remained grossly swollen at 6 weeks post-operatively with dilated lymphatics and evidence of dermal fibrosis (not shown).(6, 7) Additionally, distal regions of the tail exposed to lymphatic fluid stasis, including segments located well away from the site of lymphatic obstruction (20 and 30mm distal to the wound), had a significant increase in subcutaneous fat thickness (2-fold) as compared with proximal regions ($p<0.001$; Figure 2A–D). Although fat thickness decreased slightly in the most distal regions ($D^{+}30$) of the tail, this difference was not statistically different than the sections located closer to the wound (i.e. $D^{+}20$).

Lymph stasis results in increased number and size of lipid droplets

We performed oil red o staining of fat droplets in order to determine whether fat deposition in distal regions was due to increased fat deposition or simply hypertrophy of existing fat cells (Figure 3A, B). Interestingly, we found that regions of the tail exposed to lymph stasis had both marked hypertrophy of the fat droplets present in the subcutaneous fat layer as well as a grossly apparent increase in the number of adipocytes present.

Lymph stasis results in fibrosis of the subcutaneous fat

Trichrome immunohistochemistry stains collagen fibers blue and is a useful histological test for fibrosis. Consistent with clinical hallmarks of lymphedema, we found that regions of the tail exposed to lymphatic fluid stasis had collagen fiber deposition within the subcutaneous fat compartment (Figure 4A–C). In contrast, proximal portions of the tail had structural collagen fibers but were markedly less prominent than within distal regions.

To confirm our findings with trichrome staining, we performed collagen I immunohistochemistry. This analysis also demonstrated a marked increase in collagen deposition in the subcutaneous fat of the distal regions of the tail as compared with the proximal portions (Figure 4D–G). Interestingly, we also saw evidence of collagen fiber deposition around collecting lymphatic vessels in the distal regions of the tail (Figure 4G). This finding is consistent with histological changes noted in cadaver studies of a patient who had undergone axillary lymph node dissection.(10)

Lymph stasis results in inflammation in the subcutaneous fat

Lymphedema is clinically associated with chronic inflammation. In addition, inflammation is known to play an important role in the regulation of fat differentiation, obesity, and insulin resistance. Therefore, to study the effects of lymphatic fluid stasis on subcutaneous fat inflammation, we localized leukocytes using an antibody directed against CD45, a pan-leukocyte cellular marker. Interestingly, we found evidence of a significant inflammatory reaction in the distal regions of the tail exposed to lymphatic fluid stasis (Figure 5). Examination of proximal regions of the tail demonstrated a scant number of leukocytes in the subcutaneous fat. These cells were primarily mononuclear cells, although an occasional cell with multiple nuclei consistent histologically with polymorphonuclear macrophages were also present (Figure 5A). In contrast, subcutaneous fat in the distal region of the tail was infiltrated with a marked mononuclear cell inflammatory cell infiltrate with a more than 5-fold increase as compared to the proximal region (Figure 5B, C; $p<0.001$).

Macrophages are known to play an important role in lymphangiogenesis by producing lymphangiogenic cytokines and by differentiating into lymphatic endothelial cells.(11) In addition, macrophages are critical regulators of adipose tissue inflammation in obesity.(12)

Therefore, we localized macrophages and monocytes by staining for the macrophage/monocyte marker F4/80. This analysis, similar to our findings with CD45, demonstrated a more than 3-fold increase in the number of macrophages and monocytes in the subcutaneous fat of the distal tail regions exposed to lymphatic fluid stasis (Figure 6A–C; $p<0.001$). Again, the majority of the cells present were mononuclear cells consistent with monocytes; however, clusters of polymorphonuclear macrophages could also be seen surrounding subcutaneous fat deposits.

Discussion

Fat accumulation and fibrosis are clinical hallmarks of lymphedema.(13, 14) In the current study, we show that lymphatic obstruction in the mouse-tail model also results in significant fat deposition in the subcutaneous compartment resulting from hypertrophy and increased number of adipocytes. Further, we show that hypertrophic adipose tissues and collecting lymphatics in the mouse tail have collagen deposition consistent with fibrosis. These findings suggests that the pathologic changes that occur in this model closely resemble the clinical findings of lymphedema and enable analysis of the molecular changes that occur in response to sustained lymphatic fluid stasis. In addition, our findings of fat hypertrophy and increased number of adipocytes suggests that the process of fat accumulation in an isolated extremity in response to lymphatic fluid stasis mimics the events that occur in obesity in general.(15)

It is important to note, however, that the mouse tail, similar to the vast majority of animal models of lymphedema is not a model of lymphedema but rather a model of *sustained lymphatic fluid stasis* since the tail wound eventually heals, and in our studies, edema improves after approximately 16 weeks (unpublished observations). There are several reasons why this distinction is important and why it is unlikely that simple animal models of lymphedema can ever be developed. One major problem with animal models is the timing of lymphedema development. Clinically, lymphedema rarely develops immediately after surgery. In fact, the development of lymphedema is typically delayed, occurring on average 6–12 months after surgery.(16) Further, although clinically lymphedema is common after lymph node dissection, not every patient goes on to develop lymphedema. In fact, some patients go on to develop lymphedema after seemingly trivial lymphatic injury resulting from sentinel lymph node biopsy.(17) Taken together, these clinical findings suggest that lymphatic injury is simply the initiating event and that additional insults are necessary for lymphedema to develop. Therefore, it is unlikely that a simple surgical animal model can result in lymphedema immediately after surgery in every animal treated. The findings of the current study, however, demonstrate that tail skin and collecting lymphatic vessel ablation in the mouse tail result in lymphatic fluid stasis and histological changes that closely correlate with clinical findings of lymphedema.

Chronic lymphedema results in fibrosis of the skin and subcutaneous tissues. Further, recent clinical studies have shown that collecting lymphatic vessels become fibrosed and dysfunctional.(18) As a result of these pathological changes, patients with advanced lymphedema are thought to be poor candidates for surgical procedures that aim to restore interstitial fluid flow in the limb (i.e. lymphatic bypass procedures) since the fibrosed lymphatics are occluded and also due to the fact that the pathological changes in the skin and subcutaneous tissues may become irreversible.(19) These clinical findings implicate fibrosis as a key contributor to the etiology of lymphedema and support our previous findings demonstrating that fibrosis is a significant regulator of lymphatic function.(6–8) Our current study also supports this hypothesis as it further demonstrates that fibrosis is not only limited to the dermis but also the underlying subcutaneous tissues and collecting

lymphatics. Therefore, anti-fibrotic approaches may be a useful means of treating or preventing lymphedema.

Adipocytes develop from pluripotential mesenchymal stem cell precursors (20) and adipogenesis is dependent on environmental cues including hormones, cell-cell signaling, and cell-matrix interaction. The results of our study suggest that interactions or gradient of interstitial fluid stasis can also regulate adipogenesis. (21) This hypothesis is supported by the finding that preadipocytes *in vitro* differentiate more completely if lymphatic fluid is included in their culture media.(21) In addition, this hypothesis is supported by the fact that adipose tissue is always found surrounding lymphatic structures and that these deposits are largely resistant to caloric intake (i.e. they are maintained even in very lean individuals) but undergo lipolysis when stimulated with lymphoid derived cytokines such as tumor necrosis factor-alpha (TNF-α) and interleukin-6 (IL-6).(22) Taken together, our results and these previous studies suggest that adipose tissues interact with lymphoid tissues, may serve as an important local energy depot, and can adapt to physiologic changes in the local environment.

Obesity is associated with low-grade local inflammatory response in adipose tissues (23, 24) and inflammation has been shown to play a critical role in the development of insulin resistance.(25) The inflammatory cell infiltrate in obese adipose tissue is made up of a number of different cell types including T cells, monocytes, and macrophages.(12, 23, 26, 27) In this study we found that adipose tissue generated in response to lymphatic fluid stasis was also associated with a marked inflammatory response. We noted that the inflammatory cells in this region were primarily mononuclear cells aggregated around adipocytes. We have previously shown that lymphatic fluid stasis in the mouse tail model results in accumulation of CD4+ cells and increased expression of inflammatory cytokines such as interferon-gamma, interleukin-4, and interleukin-13.(8) It is therefore possible that T cell infiltration in response to lymphatic fluid stasis leads to expression of these inflammatory cytokines and promotes recruitment and differentiation of macrophages. This hypothesis is supported by the findings of Nishimura *et. al.* who showed that T cell recruitment in obesity precedes macrophage infiltration, and that depletion of T cells decreased macrophage accumulation and expression of inflammatory cytokines.(28) This hypothesis is also supported by the finding that high fat diets promote interferon-gamma expression in adipose tissue-derived T cells (29), and that loss of interferon-gamma function improves metabolic parameters of obese animals.(30)

Macrophages are a heterogenous population of cells derived from bone marrow precursors. In response to appropriate stimuli, bone marrow derived peripheral blood mononuclear cells migrate to regions of inflammation where they participate in removal of cellular debris, pathogen clearance, production of inflammatory cytokines, and antigen presentation. Resident tissue macrophages are also present in most tissues and contribute to normal tissue turnover and homeostasis. Obese adipose tissue is infiltrated by macrophages as evidenced by gene expression profiling and immunohistochemical localization with the macrophage marker F4/80.(23, 24) Adipose tissue macrophages and adipose tissue interact and produce a large number of pro-inflammatory mediators such as interleulin-1β, interleukin-6, and adiponectin.(15, 6, 7) Although the mechanism by which obese white adipose fat tissue induces macrophage chemotaxis is unknown, a number of hypotheses have been proposed. One possibility is that macrophages are recruited to remove adipocyte cell debris resulting from cellular necrosis. This hypothesis is supported by the finding that the majority of adipose tissue macrophages appear to be localized to regions of necrotic adipocytes forming syncytia that sequester and ingest adipocyte debris.(31) A similar mechanism may also be present in lymphatic stasis-induced adipogenesis as evidenced by our finding of nests of F4/80+ cells surrounding regions of subcutaneous fat deposition. Another potential mechanism is enhanced expression of hypoxia inducible factor-1 alpha (HIF-1α) resulting

from fat hypertrophy and insufficient blood supply.(32) This hypothesis is supported by recent studies in our lab demonstrating that lymphatic stasis is associated with significant and prolonged expression of HIF-1α (unpublished observations).

In conclusion, we have shown that lymphatic fluid stasis results in subcutaneous fat deposition in the mouse tail model and that this effect is associated with increased adipocyte number, lipid accumulation, and fibrosis. This model therefore provides an excellent means to study the molecular mechanisms that regulate the pathophysiology of lymphedema.

Acknowledgments

Sources of funding for this work are gratefully acknowledged and include an NIH T32 grant for JCZ, Society of Memorial Sloan-Kettering Grant for salary support for SE and SA, Plastic Surgery Education Foundation Research Fellowship Grants for JCZ and TA, and the Sloan-Kettering Institute Department of Surgery.

References

1. Hayes SC, Janda M, Cornish B, et al. Lymphedema after breast cancer: incidence, risk factors, and effect on upper body function. J Clin Oncol. 2008; 26:3536–3542. [PubMed: 18640935]
2. Beesley V, Janda M, Eakin E, et al. Lymphedema after gynecological cancer treatment: prevalence, correlates, and supportive care needs. Cancer. 2007; 109:2607–2614. [PubMed: 17474128]
3. Petrek JA, Senie RT, Peters M, et al. Lymphedema in a cohort of breast carcinoma survivors 20 years after diagnosis. Cancer. 2001; 92:1368–1377. [PubMed: 11745212]
4. Shih YC, Xu Y, Cormier JN, et al. Incidence, treatment costs, and complications of lymphedema after breast cancer among women of working age: a 2-year follow-up study. J Clin Oncol. 2009; 27:2007–2014. [PubMed: 19289624]
5. Ahmed RL, Prizment A, Lazovich D, et al. Lymphedema and quality of life in breast cancer survivors: the Iowa Women's Health Study. J Clin Oncol. 2008; 26:5689–5696. [PubMed: 19001331]
6. Clavin NW, Avraham T, Fernandez J, et al. TGF-beta1 is a negative regulator of lymphatic regeneration during wound repair. Am J Physiol Heart Circ Physiol. 2008; 295:H2113–2127. [PubMed: 18849330]
7. Avraham T, Clavin NW, Daluvoy SV, et al. Fibrosis is a key inhibitor of lymphatic regeneration. Plast Reconstr Surg. 2009; 124:438–450. [PubMed: 19644258]
8. Avraham T, Daluvoy S, Zampell J, et al. Blockade of Transforming Growth Factor-{beta}1 Accelerates Lymphatic Regeneration during Wound Repair. Am J Pathol. 2010; 177:3202–3214. [PubMed: 21056998]
9. Zampell JC, Yan A, Avraham T, et al. Temporal and spatial patterns of endogenous danger signal expression after wound healing and in response to lymphedema. Am J Physiol Cell Physiol. 2011
10. Suami H, Pan WR, Taylor GI. Changes in the lymph structure of the upper limb after axillary dissection: radiographic and anatomical study in a human cadaver. Plast Reconstr Surg. 2007; 120:982–991. [PubMed: 17805128]
11. Maruyama K, Ii M, Cursiefen C, et al. Inflammation-induced lymphangiogenesis in the cornea arises from CD11b-positive macrophages. J Clin Invest. 2005; 115:2363–2372. [PubMed: 16138190]
12. Harford KA, Reynolds CM, McGillicuddy FC, et al. Fats, inflammation and insulin resistance: insights to the role of macrophage and T-cell accumulation in adipose tissue. Proc Nutr Soc. 2011:1–10.
13. Altorfer J, Hedinger C, Clodius L. Light and electron microscopic investigation of extremities of dogs with experimental chronic lymphostasis. Folia Angiol. 1977; 25:141.
14. Olszewski WL, Jamal S, Manokaran G, et al. Skin changes in filarial and non-filarial lymphoedema of the lower extremities. Trop Med Parasitol. 1993; 44:40–44. [PubMed: 8516632]
15. Rosen ED. The molecular control of adipogenesis, with special reference to lymphatic pathology. Ann N Y Acad Sci. 2002; 979:143–158. discussion 188–196. [PubMed: 12543724]

16. Norman SA, Localio AR, Potashnik SL, et al. Lymphedema in breast cancer survivors: incidence, degree, time course, treatment, and symptoms. J Clin Oncol. 2009; 27:390–397. [PubMed: 19064976]

17. McLaughlin SA, Wright MJ, Morris KT, et al. Prevalence of lymphedema in women with breast cancer 5 years after sentinel lymph node biopsy or axillary dissection: objective measurements. J Clin Oncol. 2008; 26:5213–5219. [PubMed: 18838709]

18. Suami H, Taylor GI, Pan WR. The lymphatic territories of the upper limb: anatomical study and clinical implications. Plast Reconstr Surg. 2007; 119:1813–1822. [PubMed: 17440362]

19. Demirtas Y, Ozturk N, Yapici O, et al. Supermicrosurgical lymphaticovenular anastomosis and lymphaticovenous implantation for treatment of unilateral lower extremity lymphedema. Microsurgery. 2009; 29:609–618. [PubMed: 19399890]

20. Pittenger MF, Mackay AM, Beck SC, et al. Multilineage potential of adult human mesenchymal stem cells. Science. 1999; 284:143–147. [PubMed: 10102814]

21. Nougues J, Reyne Y, Dulor JP. Differentiation of rabbit adipocyte precursors in primary culture. Int J Obes. 1988; 12:321–333. [PubMed: 3198310]

22. Mattacks CA, Pond CM. Interactions of noradrenalin and tumour necrosis factor alpha, interleukin 4 and interleukin 6 in the control of lipolysis from adipocytes around lymph nodes. Cytokine. 1999; 11:334–346. [PubMed: 10328873]

23. Weisberg SP, McCann D, Desai M, et al. Obesity is associated with macrophage accumulation in adipose tissue. J Clin Invest. 2003; 112:1796–1808. [PubMed: 14679176]

24. Xu H, Barnes GT, Yang Q, et al. Chronic inflammation in fat plays a crucial role in the development of obesity-related insulin resistance. J Clin Invest. 2003; 112:1821–1830. [PubMed: 14679177]

25. Hotamisligil GS, Shargill NS, Spiegelman BM. Adipose expression of tumor necrosis factor-alpha: direct role in obesity-linked insulin resistance. Science. 1993; 259:87–91. [PubMed: 7678183]

26. Rausch ME, Weisberg S, Vardhana P, et al. Obesity in C57BL/6J mice is characterized by adipose tissue hypoxia and cytotoxic T-cell infiltration. Int J Obes (Lond). 2008; 32:451–463. [PubMed: 17895881]

27. Wu H, Ghosh S, Perrard XD, et al. T-cell accumulation and regulated on activation, normal T cell expressed and secreted upregulation in adipose tissue in obesity. Circulation. 2007; 115:1029–1038. [PubMed: 17296858]

28. Nishimura S, Manabe I, Nagasaki M, et al. CD8+ effector T cells contribute to macrophage recruitment and adipose tissue inflammation in obesity. Nat Med. 2009; 15:914–920. [PubMed: 19633658]

29. Winer S, Chan Y, Paltser G, et al. Normalization of obesity-associated insulin resistance through immunotherapy. Nat Med. 2009; 15:921–929. [PubMed: 19633657]

30. Rocha VZ, Folco EJ, Sukhova G, et al. Interferon-gamma, a Th1 cytokine, regulates fat inflammation: a role for adaptive immunity in obesity. Circ Res. 2008; 103:467–476. [PubMed: 18658050]

31. Cinti S, Mitchell G, Barbatelli G, et al. Adipocyte death defines macrophage localization and function in adipose tissue of obese mice and humans. J Lipid Res. 2005; 46:2347–2355. [PubMed: 16150820]

32. Ye J, Gao Z, Yin J, et al. Hypoxia is a potential risk factor for chronic inflammation and adiponectin reduction in adipose tissue of ob/ob and dietary obese mice. Am J Physiol Endocrinol Metab. 2007; 293:E1118–1128. [PubMed: 17666485]

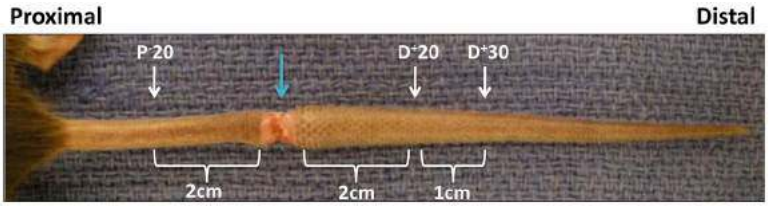

FIGURE 1. Mouse tail model of lymphatic fluid stasis

Representative photomicrograph of a mouse tail 6 weeks after lymphatic ligation. The wound is marked by the blue arrow. Tissues are harvested proximal or distal to the zone of lymphatic obstruction 6 weeks after surgery.

A

B

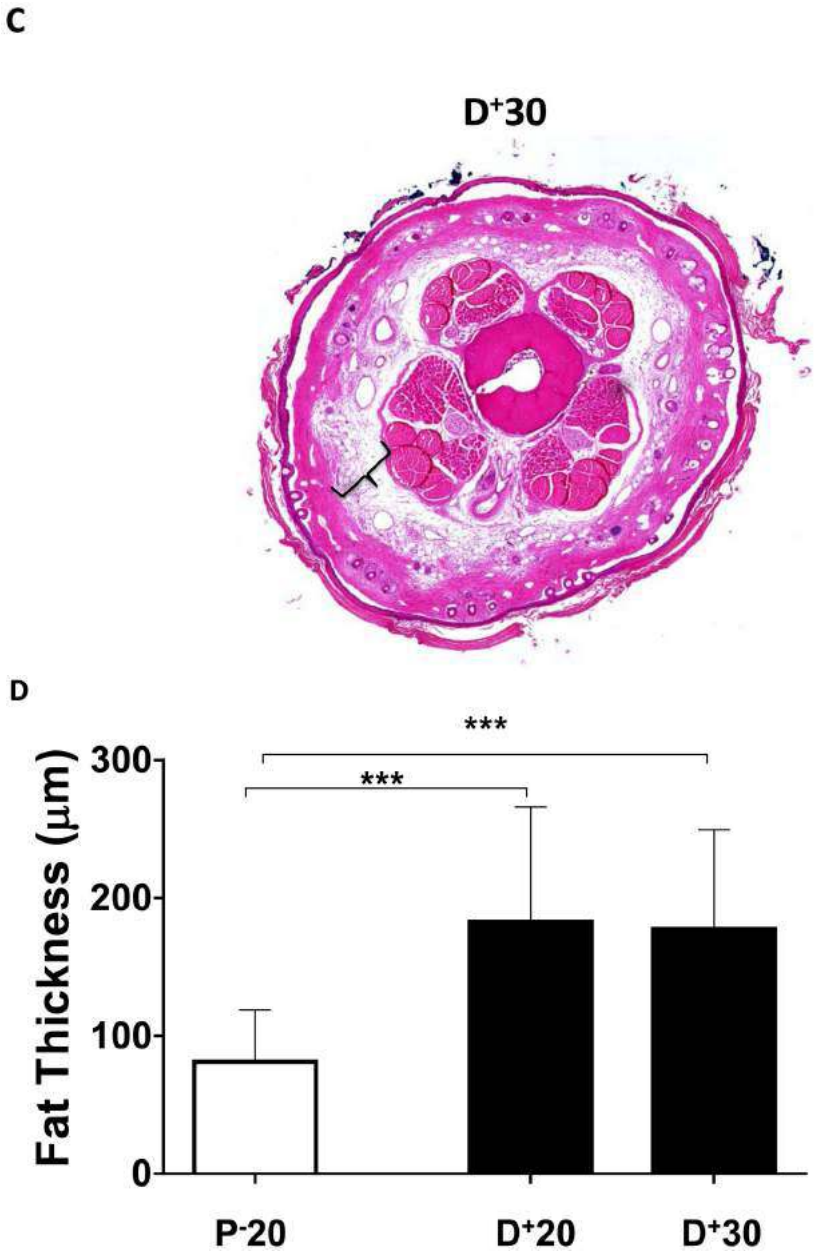

FIGURE 2. Lymph stasis increases subcutaneous fat deposition

A–C. Representative low power (2.5x) hematoxylin and eosin stain of mouse tail cross sections obtained proximal (20mm designated as $P^{-}20$) or distal (20 or 30mm designated as $D^{+}20$, $D^{+}30$, respectively) to the wound. Note marked deposition of subcutaneous fat in distal sections (indicated by brackets).

D. Quantification of fat thickness in the proximal and distal regions of the mouse tail 6 weeks after surgery. Note significant increases in fat thickness in distal regions as designated by brackets (***$p<0.001$).

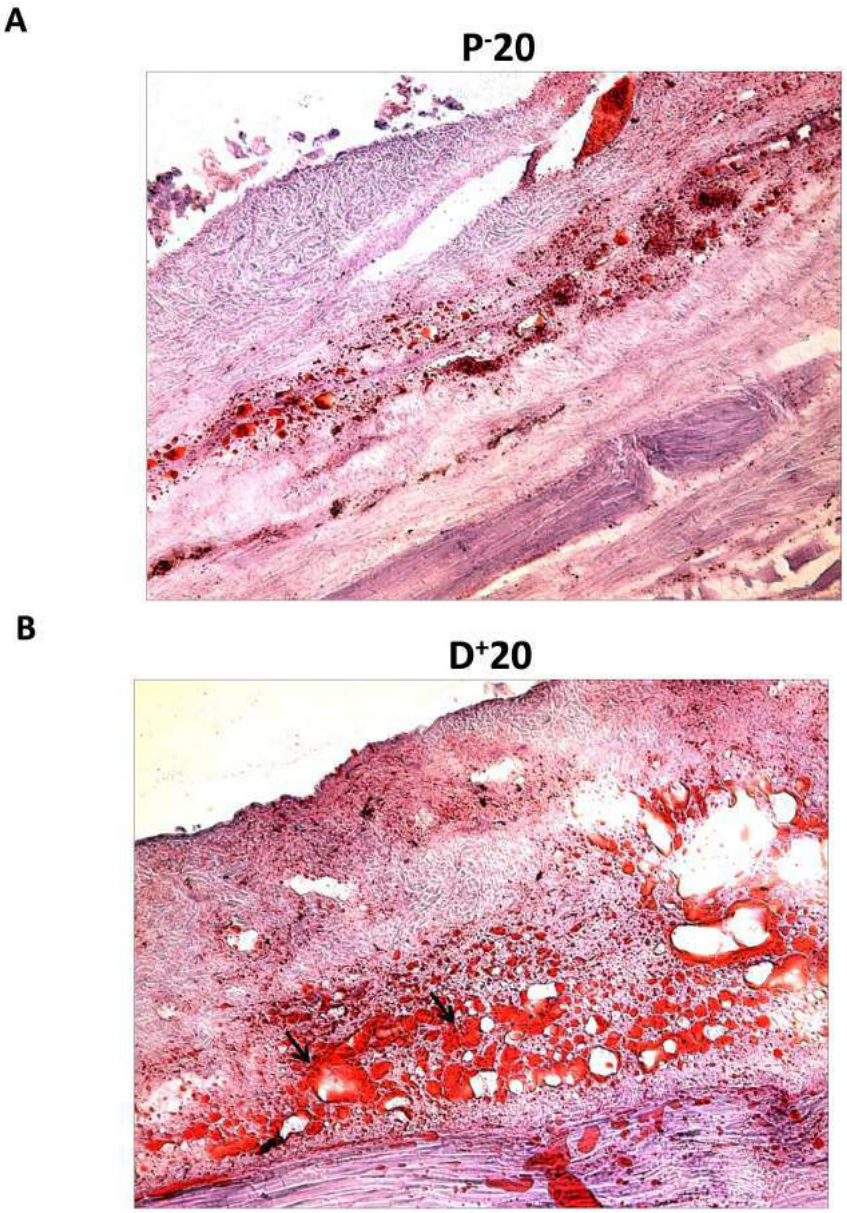

FIGURE 3. Lymph stasis results in increased number and size of lipid droplets

Representative (10x) photomicrograph of proximal and distal portions of the tail stained with oil red o. Arrows show adipocytes filled with oil red o stain. Note both increased number and hypertrophy of adipocytes in distal sections.

A

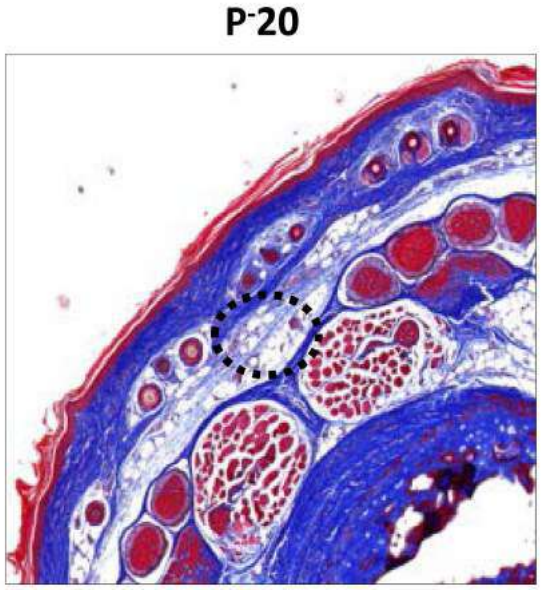

B

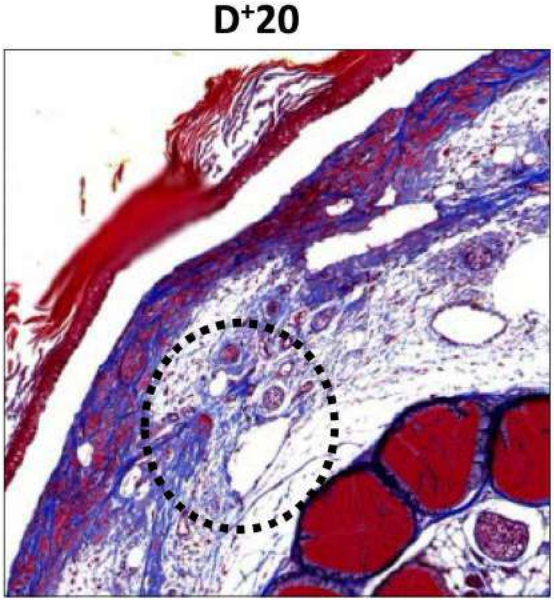

C

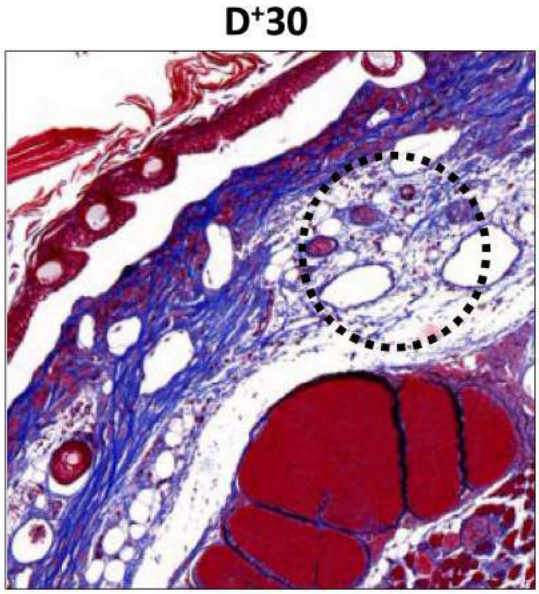

D

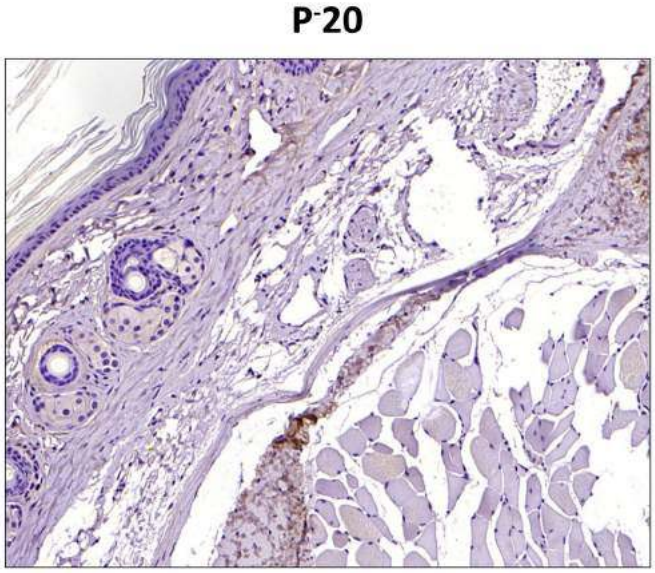

E

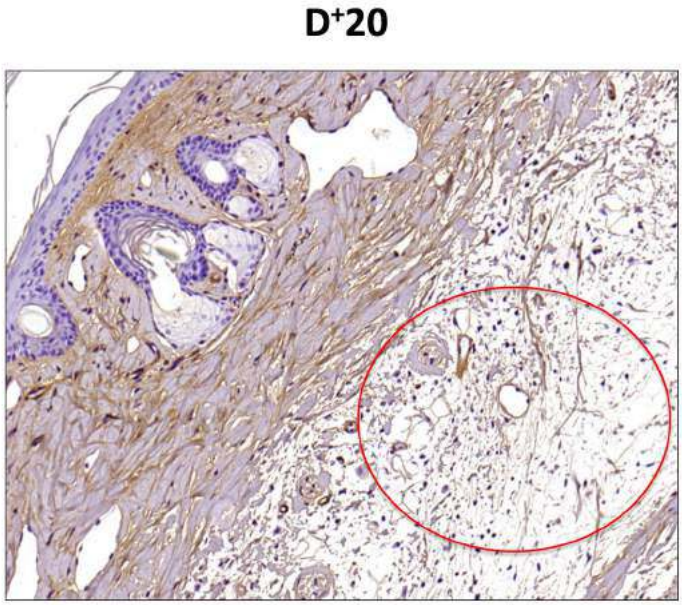

F

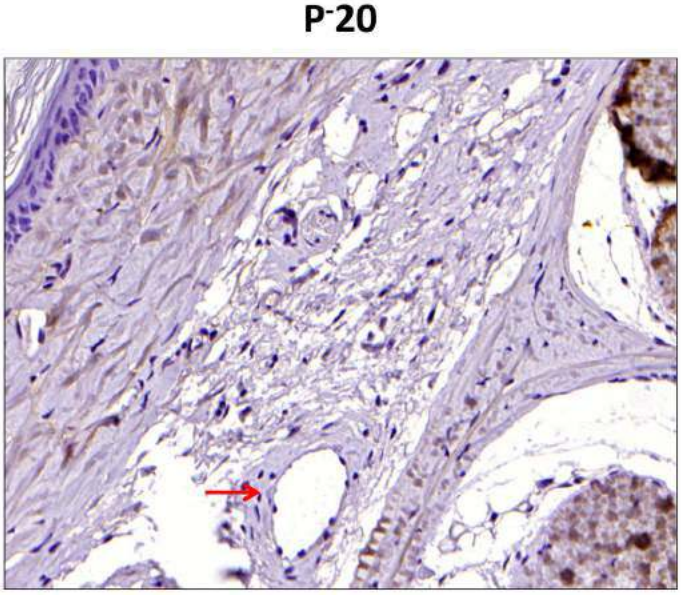

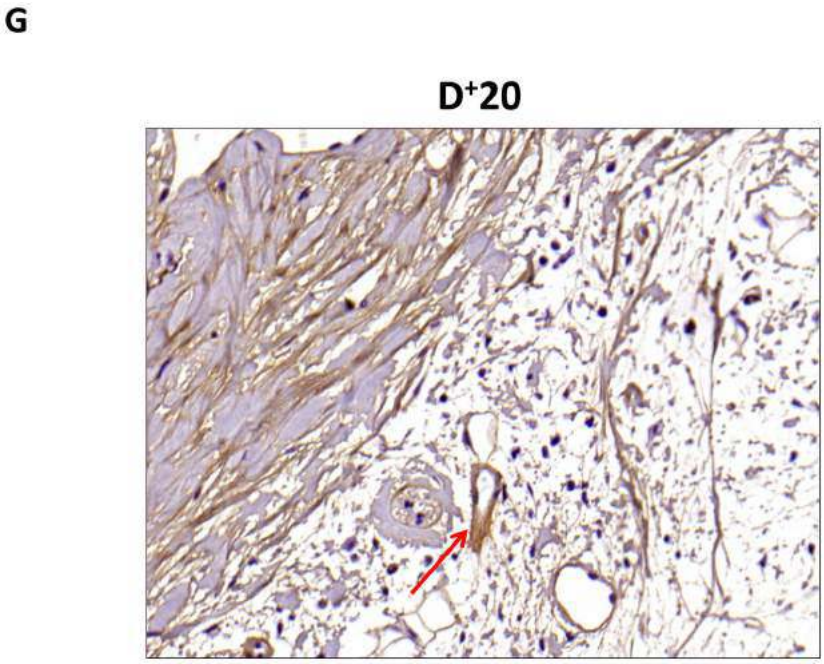

FIGURE 4. Lymph stasis results in fibrosis of the subcutaneous fat

A–C. Representative (10x) trichrome stain of mouse tail cross sections obtained proximal ($P^{-}20$) or distal ($D^{+}20$ or $D^{+}30$) to the wound. Note marked increase in collagen deposition (blue staining) in subcutaneous layer of distal region (denoted by dashed black circle).

D–G. Representative low- (10x) and high- (20x) power images of collagen I staining in proximal and distal regions of the tail. Note marked increase in dermal and subcutaneous fat collagen type I deposition in distal region seen in C and D (denoted by dashed red circle in E). Also note collecting lymphatic vessel with collagen type I staining in G (red arrow in distal photomicrograph). In contrast, note lack of collagen staining in proximal lymphatic (red arrow in proximal photomicrograph shown in F).

A

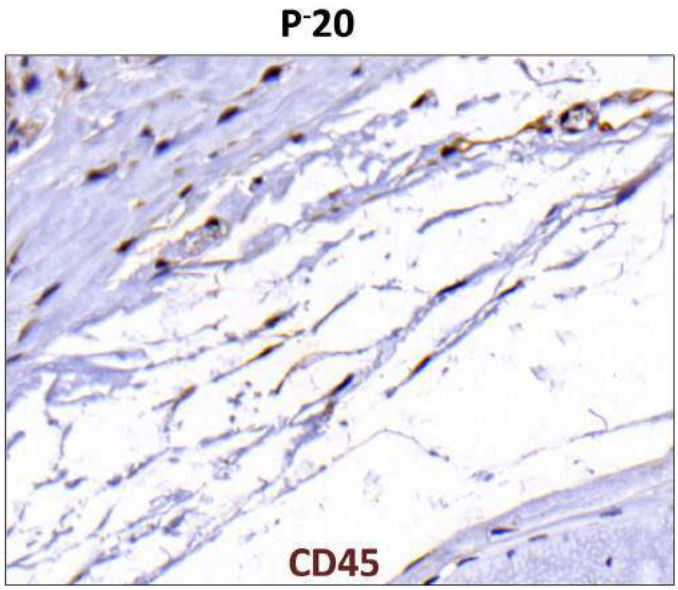

B

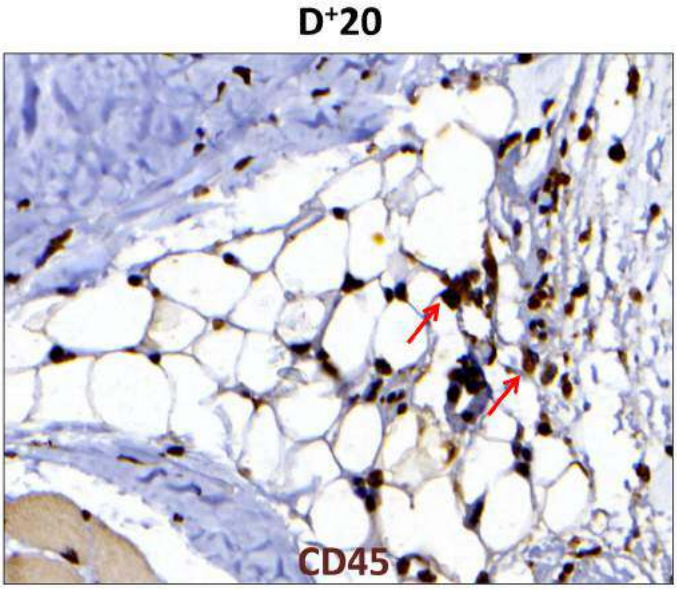

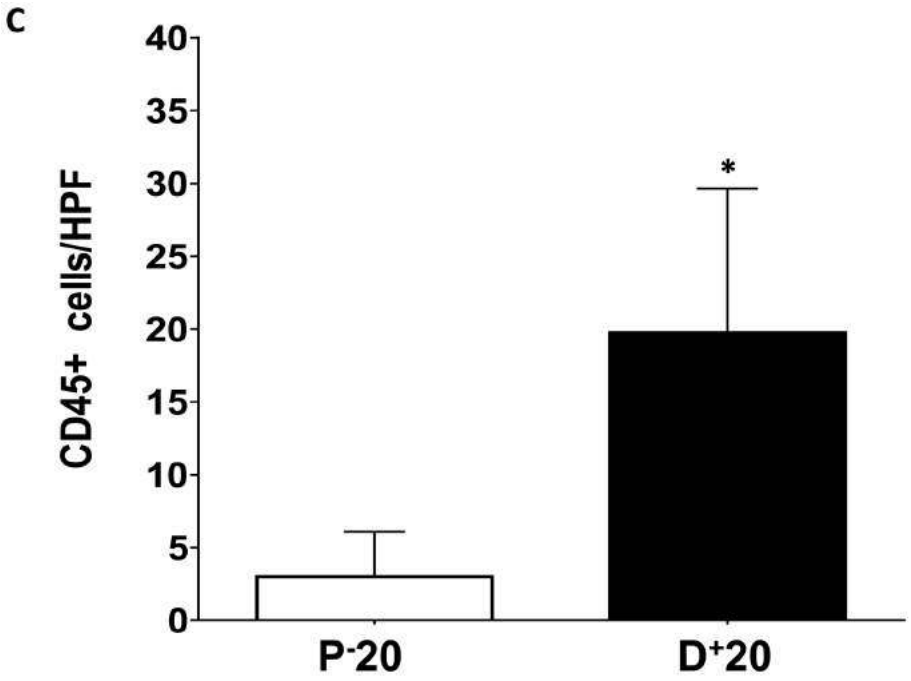

FIGURE 5. Lymph stasis results in accumulation of CD45+ mononuclear cells in the subcutaneous fat

A, B. Representative photomicrograph of proximal and distal regions of the tail after immunohistochemical localization of the pan-leukocyte marker CD45. Note marked increase in inflammation in distal segment (red arrows show positively stained cells).

C. Quantification of CD45+ cells/HPF in proximal and distal regions of the tail (*$p<0.001$).

A

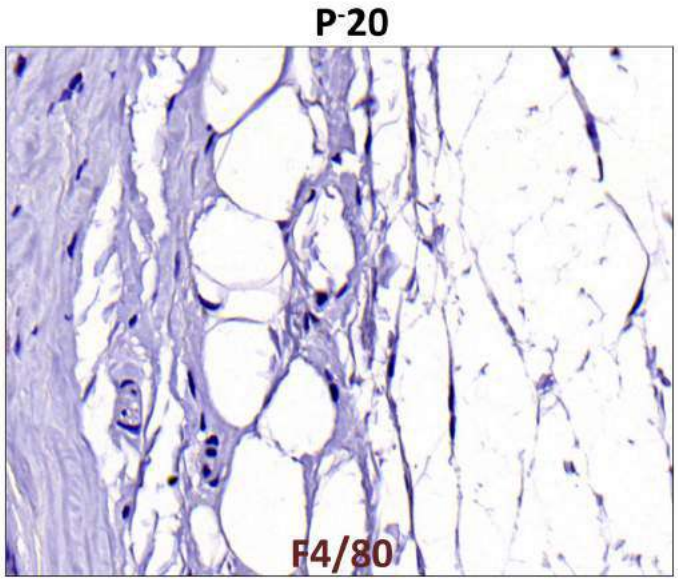

B

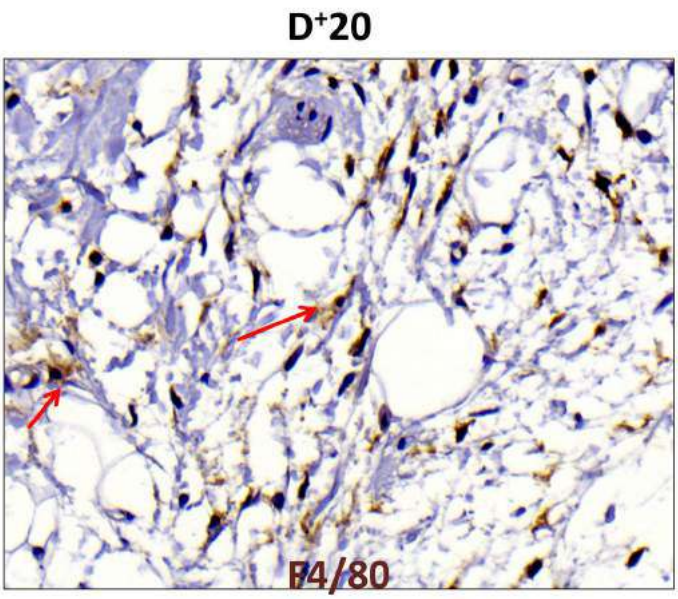

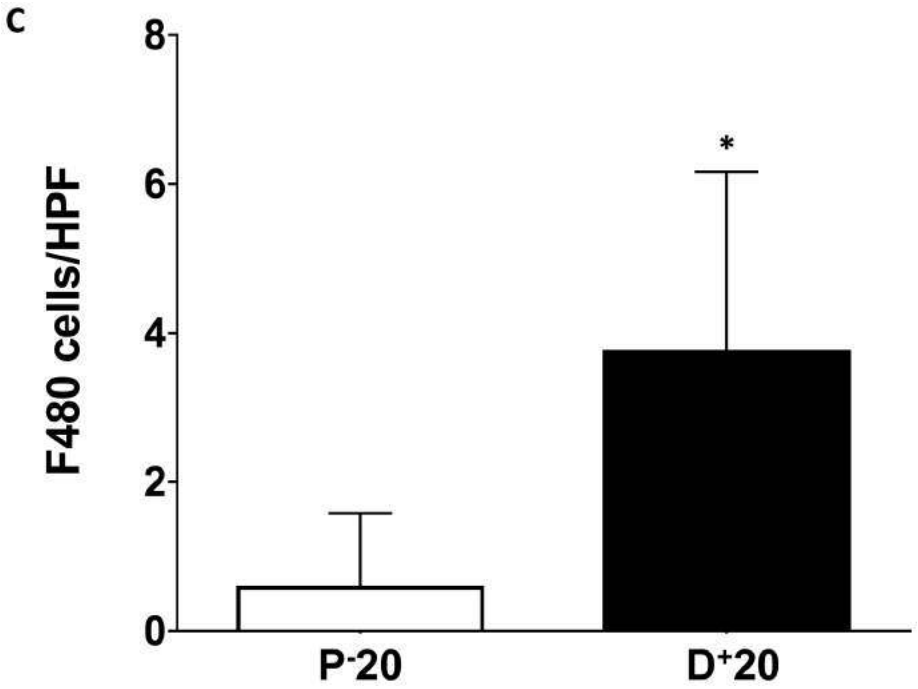

FIGURE 6. Lymph stasis results in accumulation of F4/80+ cells in the subcutaneous fat

A, B. Representative photomicrograph of proximal and distal regions of the tail after immunohistochemical localization of the monocyte/macrophage marker F4/80. Note marked increase in the number of positively stained cells in distal segment (red arrow show positively stained cells). Also note cluster of macrophages surrounding adipocytes (filled red arrow).

C. Quantification of F4/80+ cells/HPF in proximal and distal regions of the tail (*$p<0.001$).